JOURNAL OF GEOPHYSICAL RESEARCH, SPACE PHYSICS VOL. 73, NO. 3 FEBRUARY 1, 1968

Interpretation of Auroral Hiss Measured on OGO 2 and at Byrd Station in Terms of Incoherent Cerenkov Radiation

T. STOCKFLET JØRGENSEN[1]

Radioscience Laboratory, Stanford University
Stanford, California 94305

A wideband noise known as auroral hiss is observed at very low and low frequencies at ground-based stations and on satellites at high magnetic latitudes. Several attempts have been made to explain this noise as incoherent Cerenkov radiation from energetic particles in the magnetosphere, but the conclusions were all negative, as the calculated power was several orders of magnitude below the observed power. The results of recent observations of auroral hiss and of the low-energy electrons with which this noise is strongly correlated suggest that unrealistic models were used in earlier calculations of the total power generated in the magnetosphere by an incoherent Cerenkov process. Therefore it is considered worthwhile to study the Cerenkov radiation again. This paper discusses a model for a region in space in which the auroral hiss is believed to be generated. It is shown that the total power generated in this region is comparable to the observed power, and it is concluded that auroral hiss may be generated by incoherent Cerenkov radiation from electrons with energies of the order of 1 kev.

1. INTRODUCTION

During the last decade several mechanisms have been proposed as explanation of VLF and LF emissions, which are believed to originate in the earth's magnetosphere, but none of the mechanisms has ever been proved. Reviews of VLF emission theories have been given by *Helliwell* [1965, 1966].

One of the more 'popular' mechanisms was the Cerenkov process, which also was the first mechanism ever suggested as an explanation of VLF emissions [*Ellis*, 1957], but Ellis, *Liemohn* [1965], and others concluded that the total energy produced by an incoherent Cerenkov radiation process was several orders of magnitude too low to explain the observed power densities.

In view of the better information we have today of the magnetospheric environment, as well as the occurrence in space and the intensity of VLF and LF emissions compared with the situation a few years ago, it is clear that there may exist several reasons for the discrepancies between theory and observations in earlier attempts to explain emissions by Cerenkov radiation. For example, no data on the thermal electron concentration above the $F2$-layer maximum were available when Ellis did his work in 1957, and only little was known about the population of energetic particles in the magnetosphere.

Liemohn [1965] derived expressions for the power radiated by an electron spiraling in a magnetoplasma, and estimated the total power produced by energetic electrons in a tube of lines of force. The total power from an incoherent process was calculated by the expression

$$P_{\text{total}} = P_e \cdot N_e \cdot V$$

Where P_e is the average emitted power per electron, N_e is the density of the energetic electrons, and V is the volume of the tube. Assuming the direction of energy flow was strictly along the field lines, the calculated power was compared with an observed power, and it was found that the observed power exceeded the calculated power by seven orders of magnitude. This difference is much too large for the following three reasons. (1) The observed power with which the calculated power was compared was claimed to be 10^{-10} w m^{-2} Hz^{-1}, but in a recent paper *Gurnett* [1966] reports the maximum spectral density observed by Injun 3 during the satellites 10-months lifetime to be about 10^{-19} w m^{-2} Hz^{-1}, and preliminary results obtained by the VLF experiment in the OGO 2 satellite,

[1] Present address: Department of Geophysics, Meteorological Institute, Charlottenlund, Denmark.

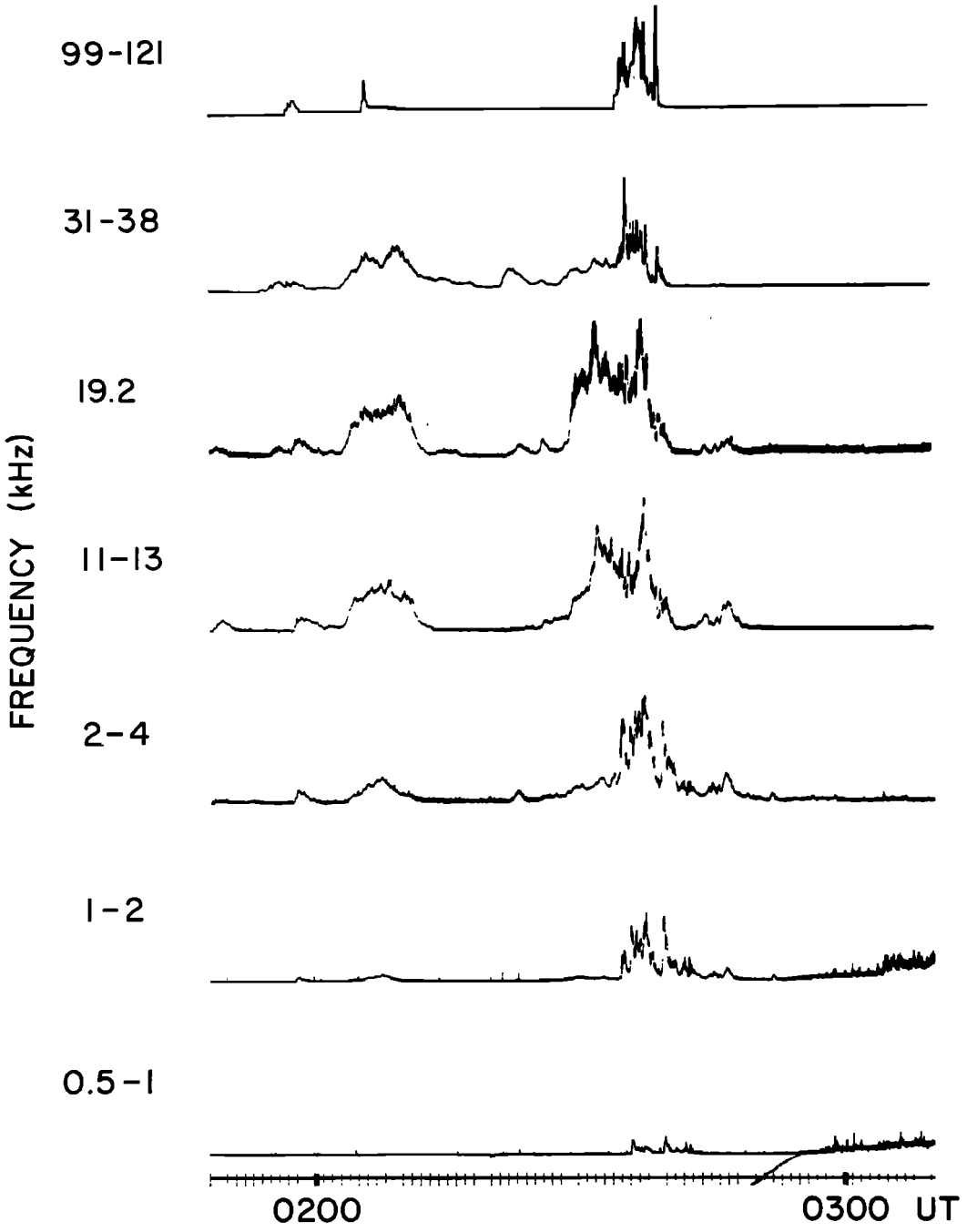

Fig. 1. Auroral hiss, Byrd Station, July 8, 1965. Amplitude (arbitrary units) as function of frequency and universal time.

which are reported in this paper, are in agreement with this. (2) Although the noise was observed at latitudes where the magnetic shell parameter L [*McIlwain*, 1961] is about 7 and higher [*Gurnett and O'Brien*, 1964], the tube of lines of force, the volume of which was used in the total power calculation, was located by Liemohn at $L = 3$, and so the volume used was much too small. (3) The density of the energetic particles was taken to be 0.1 cm^{-3}, but densities of electrons with energies between 1 and 10 kev observed in the auroral zone have been found to be almost 2 orders of magnitude higher [*Evans*, 1966].

In view of the factors discussed above, the models used in earlier works considering Cerenkov radiation as a mechanism for VLF and LF emissions probably were unrealistic, and so a new attempt is considered worthwhile.

There is no reason to believe that all types of emissions are generated by the same process, and in this paper we will consider exclusively wideband emissions above 1 kHz of the hiss type that are observed in and near the auroral zones.

First, new experimental information on hiss will be presented, and it, together with older hiss observations and other kinds of magnetospheric measurements, is the basic evidence on which we will try to determine the region in space in which hiss is generated. Then Cerenkov radiation in the magnetosphere will be discussed, and a numerical calculation of the power produced will be carried out.

2. Observations of High-Latitude Noise Emissions above 1 kHz

An amplitude-versus-time recording of a typical hiss event as it is often observed on the ground at high latitudes is shown in Figure 1. While the lower cutoff frequency of a hiss burst is of the order of 1 kHz, the upper cutoff frequency is not known. Hiss is often observed at 500 kHz at Byrd Station located in the southern auroral zone, but there may be hiss at still higher frequencies. The event shown in Figure 1 depicts clearly the wideband character of auroral hiss.

The spectral density, as a function of frequency and time, of an ordinary hiss burst in the beginning of an event also observed from Byrd Station is shown in Figure 2. It is seen

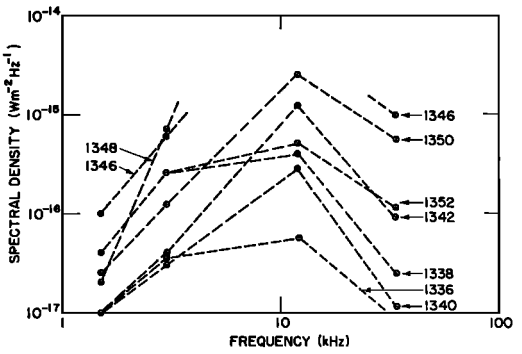

Fig. 2. Auroral hiss, Byrd Station, August 3, 1966. Spectral density as function of frequency and universal time.

that the maximum energy is received near 10 kHz.

As the spectrum may be drastically changed when the noise propagates from the magnetosphere to the surface of the earth owing to absorption and/or internal reflection in the ionosphere, it is important to know the noise spectrum observed in space. Such information has been obtained by the VLF and LF receivers in the polar-orbiting OGO 2 satellite, and is presented in Figure 3. The results of 26 passes through noise regions in both hemispheres between 65 and 82° magnetic latitude in the period November 12–23, 1965, are shown. Each two points connected by a dashed line represent spectral densities measured at two frequencies simultaneously. The satellite receivers are calibrated in terms of gammas, and the following expression has been used for conversion to w m^{-2} Hz^{-1}:

$$P = \frac{1}{\mu} \cdot 120\,\pi \cdot \frac{1}{\mu_0^2} \cdot 10^{-18} \cdot \frac{\gamma^2}{B} \text{ (w m}^{-2}\text{ Hz}^{-1}\text{)}$$

where μ is the refractive index, μ_0 is the magnetic permeability of free space $= 4\pi \cdot 10^{-7}$ h/meter, γ is the wave magnetic field strength in gammas, and B is the receiver bandwidth. As we do not know the wave normal direction of the received noise and the electron concentration of the plasma surrounding the satellite, the orbit of which has perigee = 412 km and apogee = 1508 km, it is assumed that μ can be reasonably well represented by the longitudinal whistler mode refractive index, and further that the electron concentration at the satellite is 10^4

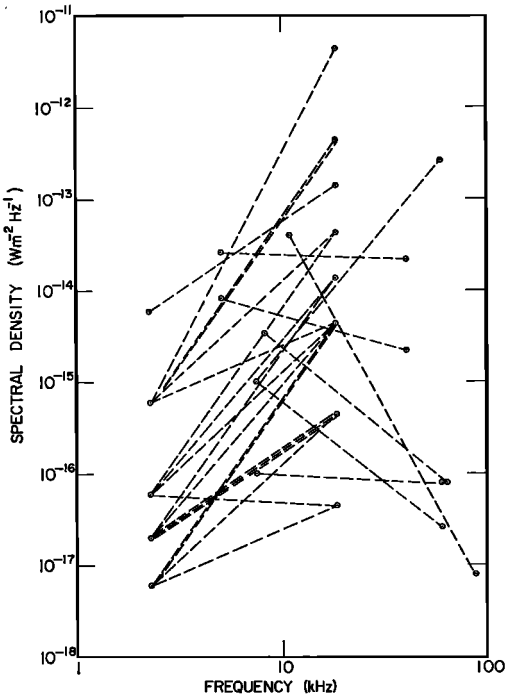

Fig. 3. Auroral hiss observed by OGO 2, November 12–23, 1965. Each dashed line corresponds to one pass of the satellite through a noise region, and the endpoints of a line represent the spectral densities measured at two frequencies simultaneously.

electrons/cm^3. (This last assumption is discussed below.)

The hiss spectrum observed by the satellite seems to have a maximum near 10 kHz similar to hiss observed on the ground. A typical average spectral density is 10^{-15}–10^{-14} w m^{-2} Hz^{-1}. Only in one case of the 26 noise region passes studied did the spectral density exceed 10^{-13} w m^{-2} Hz.

Figure 4 shows frequency-time spectrograms of hiss received simultaneously by the OGO 2 satellite and by Byrd Station during a satellite pass in zenith over Byrd. The noise observed from the satellite and from the ground roughly between 1345 UT, at which time the satellite crossed the zenith, and 1348 UT is probably the same noise, as the lower cutoff frequencies on the two recordings are seen to change with time in very smilar ways. Outside this time interval there is no correlation between the two spectrograms. Of the 25 passes of OGO 2 over the Antarctic continent randomly chosen during the period from the launching of the satellite in October 1965 to August 1966, the example shown in Figure 4 is the only one in which hiss was observed on the ground and in space simultaneously. This indicates that the satellite must be close to the zenith for the same hiss burst to be observed from the satellite as well as from the ground. The observation is consistent with ground-based observations [*Jørgensen*, 1966], which show that the region on the earth illuminated by hiss at any moment is rather small, at least in the direction of the magnetic meridian, that is of the order of a few hundred kilometers.

In Figure 5 the 25 OGO 2 broadband (0.2–12.5 kHz) recordings mentioned above are displayed in a geomagnetic latitude–geomagnetic time coordinate system. The solid, dashed, and and dot-dashed lines indicate where hiss, whistlers, and chorus were observed, respectively. Obviously hiss and whistlers occur in two different regions of the magnetosphere separated by what looks like the low-latitude boundary of the auroral zone. This boundary is apparently the same as the low-latitude boundary of the hiss zone found from ground-based hiss recordings [*Jørgensen*, 1966] and from hiss measurements by the Injun 3 satellite [*Gurnett*, 1966]. The observations of chorus are consistent with ground-based observations that have shown that chorus is a daytime phenomenon [*Helliwell*, 1965].

Thus far only the high-latitude noise emission known as auroral hiss has been discussed, but another and similar emission, the lower hybrid resonance (LHR) noise, is also observed from satellites at high latitudes.

McEwen and Barrington [1967] reported the characteristics of LHR noise observed by the Alouette 1 satellite. They classified the noise according to spectral appearance and latitudinal region of occurrence as midlatitude LHR and polar LHF. We will be interested here in the latter.

The characteristics of polar LHR as reported by *McEwen and Barrington* [1967] are as follows: (1) polar LHR is mainly observed in the region 70–85° invariant latitude; (2) it has a peak in occurrence slightly before midnight, but is observed on the day side of the earth as well; and (3) it is typically observed as a

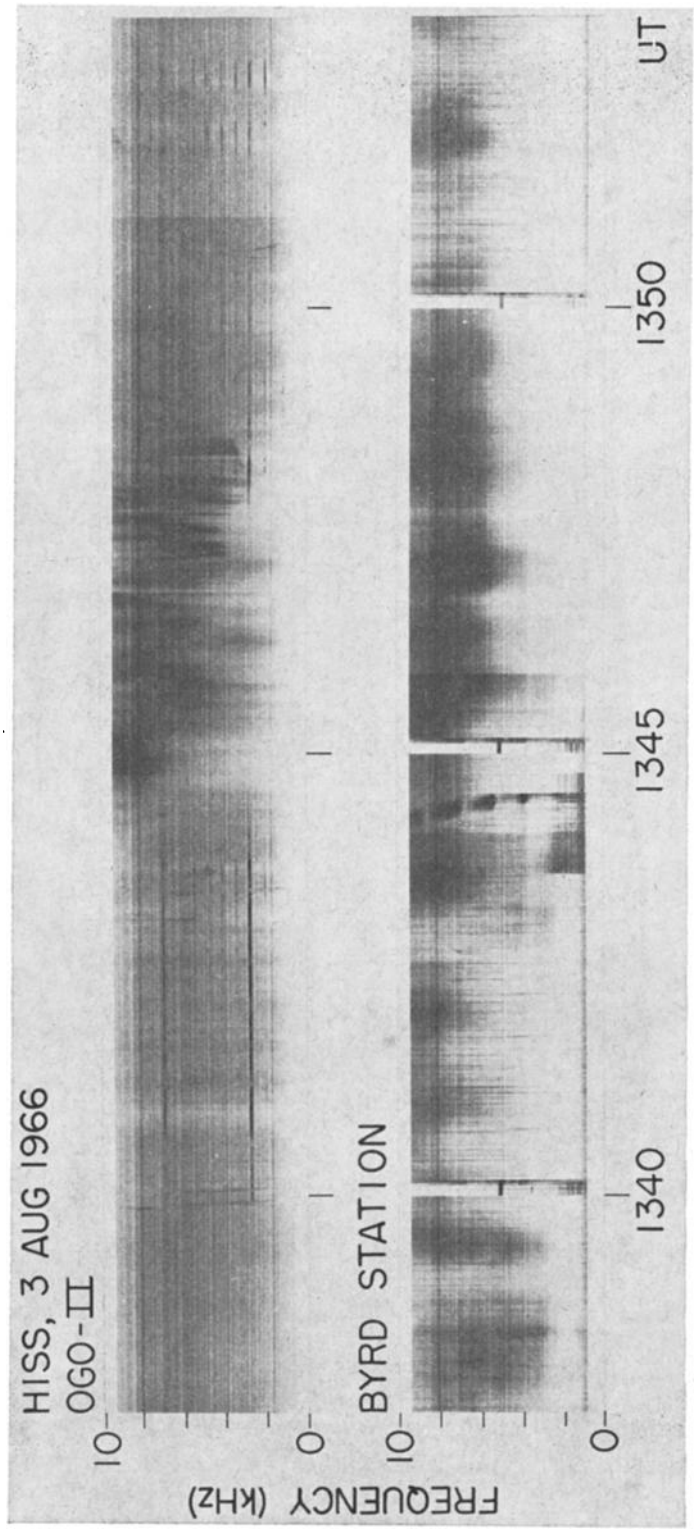

Fig. 4. Frequency-time spectrograms of auroral hiss observed simultaneously from OGO 2 and from Byrd Station, August 3, 1966. The satellite was in zenith over Byrd Station at 1345 UT.

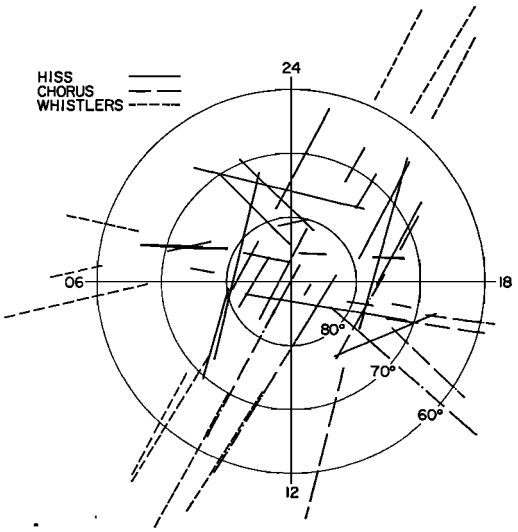

Fig. 5. Observations of hiss, whistlers, and chorus by the broadband (0.2–12.5 kHz) OGO 2 receiver plotted in a geomagnetic latitude–geomagnetic time coordinate system. The observations indicate the different regions of the magnetosphere in which the three phenomena typically occur.

noise band with relatively large bandwidth (several kHz) and a lower cutoff frequency at about 5 kHz.

This description is indistinguishable from descriptions of auroral hiss [*Gurnett*, 1966], and so it is suggested that the emission named polar LHR by some workers is equivalent to the emission called auroral hiss by others.

Gurnett and O'Brien [1964] and *Gurnett* [1966] found that intense fluxes of soft electrons often are accompanied by hiss. It was found that the correlation between hiss and intense fluxes ($I > 2.5 \times 10^7/cm^2$ ster sec) of electrons ($E > 10$ kev) is dependent on the exponential folding energy E_0. The correlation is very good for $E_0 = 3$–4 kev, but poor for larger E_0 values.

Recently Explorer 20 topside sounder electron concentration data were compared with auroral backscatter data obtained simultaneously at College, Alaska [*Lund et al.*, 1967]. The observations show that auroral precipitation produces electron concentration fluctuations that are large in amplitude (of the order of 2x to 5x ambient) and small in geographic size (of order 1–10 km), along with a general increase in the ionospheric electron concentration within the latitudinal region containing the precipitation. It is remarkable that the low-latitude boundary of the auroral precipitation as determined from the College backscatter sounder is very similar to the low-latitude boundary of the large-amplitude, small extent, electron concentration variations detected by Explorer 20 and very similar to the low-latitude boundary of the hiss zone as well.

3. The Region of Noise Generation

Concerning the region in space in which hiss is generated, the experimental work carried out so far seems to be consistent with the following picture: Hiss is generated in the auroral regions of the magnetosphere, and the mechanism of generation is closely connected to very intense fluxes of electrons with energies of the order of a few kev. Since the energy flux of the energetic electrons is many orders of magnitude larger than the electromagnetic energy flux [*Gurnett and O'Brien*, 1964], it seems reasonable to assume that hiss is generated by the energetic electrons.

The Cerenkov mechanism that we will consider in this paper depends on plasma parameters such as gyrofrequency and plasma frequency of the thermal electrons and ions as well as the distribution function of the energetic electrons. Therefore we will now try to determine these parameters and thus make a model for the region in the magnetosphere in which hiss is believed to be generated.

The energetic particles spiral along the lines of force of the earth's magnetic field, and the energy of a whistler-mode wave propagates mainly in the direction of the magnetic field as long as the wave frequency is not too close to the electron gyrofrequency [*Helliwell*, 1965]. Therefore, it seems fair to assume that the generation takes place in a tube of lines of force that hits the surface of the earth at auroral latitudes, where the hiss activity is maximum. A suitable field line along which we can carry out our investigation would be one that hits the surface of the earth at 70° geomagnetic latitude.

Gyrofrequency. The main magnetic field of the earth can be approximated by the field due to a magnetic dipole placed at the center of the earth. In the magnetosphere, the dipole model of the earth's magnetic field is a reasonably

good one out to at least 5 R_E, and so we will consider the field line along which we want to know the electron gyrofrequency as one belonging to a dipole field.

For a dipole field we have the following expressions for determination of the electron gyrofrequency f_{He} [*Helliwell*, 1965]:

$$f_{He} = f_{Heq}\left(\frac{R_0}{R}\right)^3 (1 + 3\sin^2\phi)^{1/2}$$

$$R = R_0 \frac{\cos^2\phi}{\cos^2\phi_0}$$

Where f_{Heq} is the electron gyrofrequency at the equator at the surface of the earth = 880 kHz, R_0 is the mean earth radius = 6370, km, R is the geocentric radius, ϕ is the geomagnetic latitude, and ϕ_0 is the geomagnetic latitude at R_0. By combining the two equations we find

$$f_{He} = f_{Heq}\left(\frac{R_0}{R}\right)^3\left[1 + 3\left(1 - \frac{R}{R_0}\cos^2\phi_0\right)\right]^{1/2}$$

which gives the electron gyrofrequency along a given field line as a function of geocentric distance. In Figure 6 the gyrofrequency along the field line cutting the surface of the earth at 70° geomagnetic latitude is shown.

Plasmafrequency. The electron plasmafrequency f_0 is given by

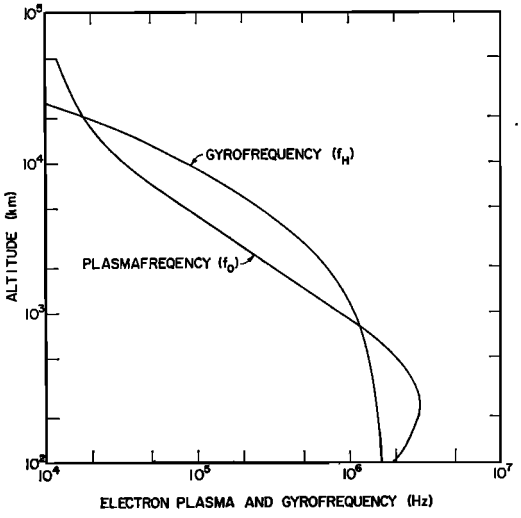

Fig. 6. Electron plasma-frequency and gyrofrequency as functions of altitude in the model region of hiss generation.

$$f_0^2 = \frac{Ne^2}{4\pi^2 m\epsilon_0}$$

Where N is the electron density, e and m are the electronic charge and mass, respectively, and ϵ_0 is the electric permittivity of free space.

While electron concentration measurements have been carried out at auroral latitudes from the bottom of the ionosphere and up to about 3000 km [*Hagg*, 1967], we more or less have to guess about the electron concentrations above 3000 km at these latitudes.

Jespersen et al. [1966] made electron concentration measurements in the lower ionosphere from Andenes in Norway close to the zone of maximum occurrence of aurora by means of rocket-borne Faraday rotation experiments. They found electron concentrations of the order of 10^4–10^5 cm^{-3} at 100 km near magnetic midnight during moderate auroral disturbances in connection with which hiss is generally observed on the ground.

Ionograms from Godhavn and Narssarssuaq, in Greenland, obtained during periods of strong hiss activity in the winter and spring months of 1964, show that the maximum plasma frequency in the F-layer varies between 2 and 4 MHz. A typical value is 3 MHz that we can use in our model ionosphere.

The information on electron concentrations in the polar magnetosphere from the F-layer maximum and up is obtained mainly from topside soundings provided by the Alouettes 1 and 2 and Explorer 20 satellites.

Concerning the electron concentration at an altitude of 1000 km [*Thomas et al.*, 1966], there exists a monotonic decrease with latitude from a few times 10^4 electrons/cm^3 at midlatitudes to as low as 10^3 electrons/cm^3 near the magnetic poles, with daytime higher than nighttime values. However, superimposed on this latitudinal distribution are prominent large-scale minima or 'troughs.' Of more importance, perhaps, is the observation that large electron concentration maxima or 'peaks' occur at latitudes greater than those at which the troughs are found. At these maxima, the electron concentration often reaches a magnitude exceeding that observed at midlatitudes. The peak-to-trough ratio of the electron concentrations at the height of the satellite may exceed 25 to 1. Both the troughs and peaks have spatial mag-

nitudes of a few hundred km. In addition, small-scale irregularities exist in space and time.

Unfortunately, as we do not have small-scale electron concentration information obtained from a satellite simultaneous with hiss intensity measurements, it is rather difficult to say what a typical electron concentration is at an altitude of about 1000 km at auroral latitudes during a hiss event, but a figure of 1×10^4 electrons/cm^3 may be representative.

Between 1000 and 10,000 km we will assume that the plasmafrequency decreases with approximately the same rate as the gyrofrequency. This so-called gyrofrequency model has been given a theoretical basis by *Dowden* [1961]. Above 10,000 km the plasmafrequency is likely to decrease asymptotically to the plasmafrequency of interplanetary space, which is of the order of 10^4 Hz. The plasmafrequency model derived as described above is shown in Figure 6.

Ion composition. Work by *Storey* [1956], *Hines* [1957], and others has shown that ions have an effect on propagation of VLF waves in the magnetosphere. Therefore, we will include the composition of positive ions in the model magnetosphere we will use in connection with the Cerenkov radiation calculations. To the author's knowledge little is known about ion composition in the high-latitude magnetosphere, so we will use information obtained at midlatitudes and assume that such results may be representative of the ion composition at auroral latitudes. From whistler studies, *Beghin* [1966] found the composition of oxygen, helium, and hydrogen ions as a function of altitude. We will use the data shown in Beghin's Figure 8*a*. Our resulting derived ion composition model is shown in Figure 7.

Energetic particles. As mentioned above, simultaneous observations by the Injun 3 satellite [*Gurnett,* 1966] of hiss and of electrons with energies larger than 10 kev showed that hiss almost always was observed when the satellite passes through very intense streams of auroral electrons. The observations indicated that electrons with energies less than 10 kev play an important role in the production of hiss.

A rather detailed investigation of the auroral electron spectrum above 1 kev has been carried out by *Evans* [1966] who flew channel multiplier detectors on two rockets through auroras over Fort Churchill. Both rockets were launched

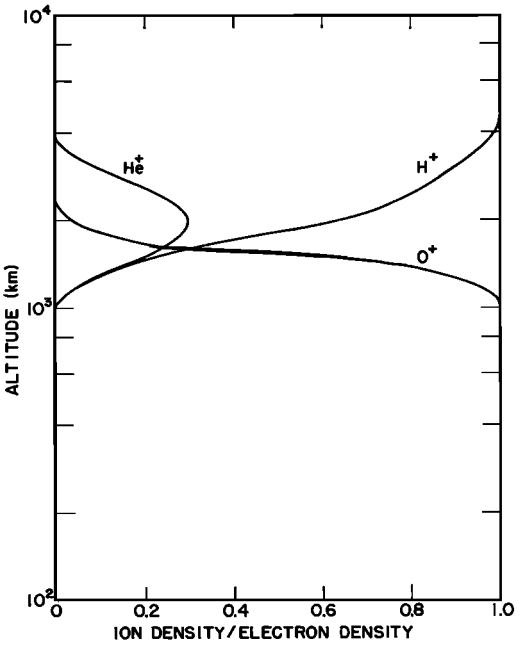

Fig. 7. Positive ion composition as function of altitude in the model region of hiss generation.

around magnetic midnight during moderately disturbed conditions, which seem to have been typical hiss conditions. It is not know if any VLF observations were made during the rocket launchings, but we will assume that the electron spectra observed by *Evans* [1966] are representative of the electron fluxes that are correlated to hiss.

An average of the spectrums observed by Evans is shown in Figure 8. The pitch-angle distribution for electrons with energies below 4 kev was reported to be nearly isotropic. Also in Figure 8 the density of the energetic electrons in the energy intervals indicated near the bottom of the figure is shown. The density of electrons with energies between 1 and 16 kev is seen to be 8 electrons/cm^3.

In the calculations of the total power produced by the Cerenkov process, which will be discussed in the next section, it will be asssumed that the density of the energetic particles is the same everywhere in the flux tube, which we consider as the region of generation of hiss. Furthermore it will be assumed that the pitch-angle distribution is isotropic.

These are probably fair assumptions owing to the fact that electron spectra, measured in

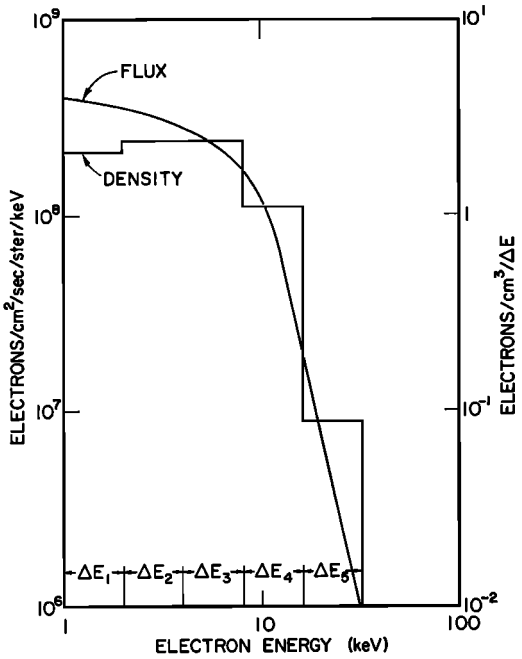

Fig. 8. Flux and density as functions of energy of auroral electrons believed to generate hiss.

the dark hemisphere of the magnetosphere at much larger distances from the earth (8–20 R_E) [*Frank*, 1967] than those we are going to consider (1–5 R_E) are very much like the spectra observed by Evans in the lower ionosphere. The electron fluxes reported by *Frank* [1967] are only about one order of magnitude below the fluxes observed by *Evans* [1966], and likewise the pitch-angle distribution is close to isotropic.

4. Cerenkov Radiation in the Whistler Mode in the Magnetosphere

A Cerenkov wave is generated by a charged particle moving in a plasma, if the component in the wave normal direction of the particle's longitudinal velocity equals the phase velocity of the wave. This means that Cerenkov radiation only can occur at frequencies for which the refractive index is greater than one, that is: (1) at frequencies above the plasma cutoff and below the upper hybrid plasma resonance; and (2) at frequencies below the plasma cutoff and below the electron cyclotron resonance. This can be seen, for example, by consideration of the α, β diagram [*Allis et al.*, 1963].

Auroral hiss is believed to propagate in the whistler mode, and in this paper we will exclusively consider Cerenkov radiation in this mode, that is to say in the second of the two frequency domains mentioned above.

Considering the variation of the electron gyrofrequency as a function of altitude in the model region of generation (Figure 6), it is clear that the maximum frequency at which Cerenkov radiation can be generated in the whistler mode is equal to the electron gyrofrequency at the bottom of the ionosphere, that is about 1.6 MHz. High frequencies can only be generated in a relatively short flux tube close to the earth, while low frequencies can be generated in a long flux tube. For example radiation at 1.0 MHz can only be generated below an altitude of 1000 km, while radiation frequencies at 10 kHz can be generated at all altitudes up to about 25,000 km.

A qualitative discussion of the properties of Cerenkov radiation in the whistler mode can be carried out using a technique shown by *McKenzie* [1963]. This technique is demonstrated in Figure 9, where the four main configurations of whistler mode refractive index surfaces are drawn for frequencies between the ion cyclotron frequency f_{H_i} and the electron cyclotron frequency f_{H_e}.

To find out if Cerenkov radiation is generated at a certain frequency by a particle with a certain longitudinal velocity $v_\parallel$, the appropriate refractive index surface is drawn, and a line of length $c/v_\parallel$, where c is the free space velocity of light, is drawn from the origin of the refractive index surface diagram, parallel to the magnetic field direction **B**. If a right triangle with two of the sides being $c/v_\parallel$ in the magnetic field direction and the refractive index μ in the wave normal direction can be constructed as shown in Figure 9, a Cerenkov wave will be emitted at the frequency in question. That this condition is equivalent to the Cerenkov condition mentioned above is easy to see from the triangle, where $\mu \cos \theta = c/v_\parallel$. The ray direction can also be found from the figure, because we know that the ray **R** is perpendicular to the refractive index surface.

As $c/v_\parallel$ is inversely proportional to the longitudinal particle velocity, it is seen that for $f_{H_i} < f \leq f_{LHR}$, where f_{LHR} is the lower hybrid resonance frequency, Cerenkov radiation can only be generated by particles with longitudinal velocities larger than a certain velocity $v_{\parallel \min}$,

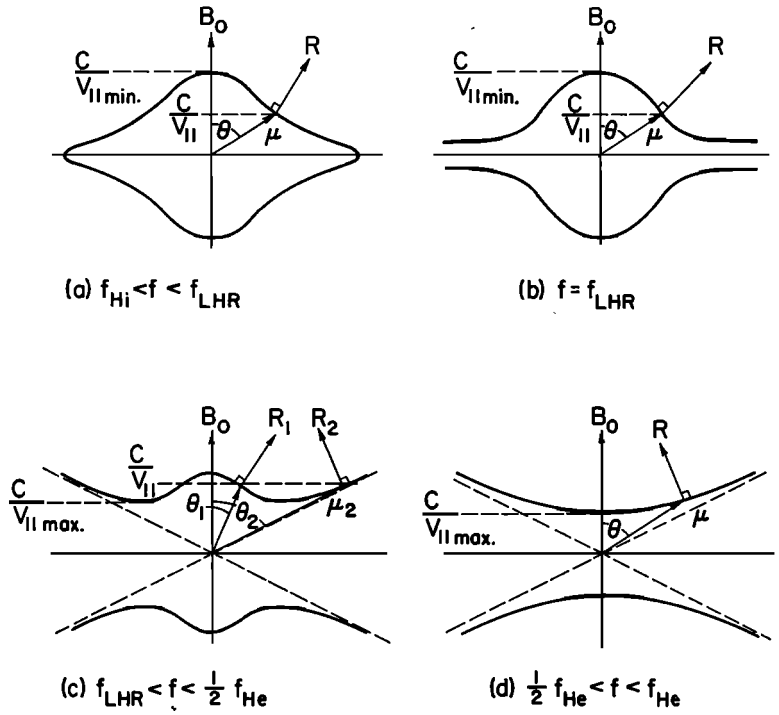

Fig. 9. The Cerenkov radiation condition in the whistler domain studied by use of refractive index surfaces. Cerenkov radiation is generated by a particle with longitudinal velocity $v_\parallel$ if a line perpendicular to the magnetic field direction $\mathbf{B}_0$ and with distance $c/v_\parallel$ from the center of the refractive index surface cuts the refractive index surface. Both the wave normal direction μ and the ray direction $\mathbf{R}$ are found by the construction. For $f_{LHR} < f < 1/2 f_{He}$, two waves with the same frequency may be generated.

whereas for $f_{LHR} < f < f_{He}$ Cerenkov radiation can occur only when the longitudinal particle velocity is less than a certain maximum velocity $v_{\parallel max}$. Considering the frequency range $f_{LHR} < f < \frac{1}{2}f_{He}$, it is seen from Figure 9c that there exists a certain particle velocity range in which two different waves will be emitted at the same frequency.

Expressions for the power produced by Cerenkov radiation from a charged particle spiraling in a cold magnetoplasma have been derived by *Mansfield* [1964] and by *Liemohn* [1965]. As we will consider only Cerenkov radiation in the magnetospheric plasma, which has a temperature corresponding to an energy less than 1 ev, generated by particles with energies greater than 1 kev, we will assume that the cold plasma theory is valid for this study.

According to *Mansfield* [1964] (whose results are in agreement with those of *Liemohn* [1965]), the power produced by Cerenkov radiation from a single particle expressed in w/Hz is given by the following equation:

$$dP/df = \sum_{i=1}^{2} q^2 2\pi f [\beta_\perp^2 T_{11} J_1^2(L_0) + \beta_\parallel^2 T_{33} J_0^2(L_0) - 2\beta_\perp \beta_\parallel T_{13} J_1(L_0) J_0(L_0)]/\epsilon_0 v_\parallel \cdot (B_n^2 - 4C_n\epsilon_1)^{1/2} \Big|_{\mu=\mu_i}$$

where

$$\beta_\perp = v_\perp/c \qquad \beta_\parallel = v_\parallel/c$$

$$B_n = (c/v_\parallel)^2(\epsilon_3 - \epsilon_1) + \epsilon_2^2 - \epsilon_1^2 - \epsilon_1\epsilon_3$$

$$C_n = (c/v_\parallel)^2(\epsilon_1^2 - \epsilon_2^2 - \epsilon_1\epsilon_3) + \epsilon_3(\epsilon_1^2 - \epsilon_2^2)$$

$$\mu_{1,2}^2 = [-B_n \pm (B_n^2 - 4C_n\epsilon_1)^{1/2}]/2\epsilon_1$$

$$\cos\theta = 1/\beta_1\mu$$

$$T_{11} = \epsilon_1\epsilon_3 - \epsilon_1\mu^2 \sin^2\theta - \epsilon_3\mu^2 \cos^2\theta$$

$$T_{13} = \epsilon_2\mu^2 \sin\theta \cos\theta$$

$$T_{33} = \epsilon_1^2 - \epsilon_2^2 - \epsilon_1\mu^2 + (\mu^4 - \epsilon_1\mu^2)\cos\theta$$

$$L_0 = (f/f_{He})\beta_\perp\mu \sin\theta$$

In these expressions q is the charge of the electron, $v_\perp$ is the particle's transverse velocity, ϵ_1, ϵ_2, and ϵ_3 are the dielectric tensor elements with the ions (Figure 7) included, θ is the wave normal angle relative to the earth's magnetic field, J_0 and J_1 are the Bessel functions of first kind and zeroth- and first-order, respectively, and L_0 is the argument of the Bessel functions. MKS units are used.

Using Mansfield's expression, the power produced at different frequencies between 1 kHz and 1 MHz by Cerenkov radiation from a spiraling electron has been calculated as a function of particle energy, pitch angle, and altitude in the model region of noise generation discussed earlier in this paper. The results of some of these calculations are shown in Figure 10 for the case of a 1-kev electron with 0° pitch angle. It is seen that the highest powers are generated at low altitudes in the upper end of the frequency band we are studying, whereas the low-frequency radiation mainly is generated at high altitudes.

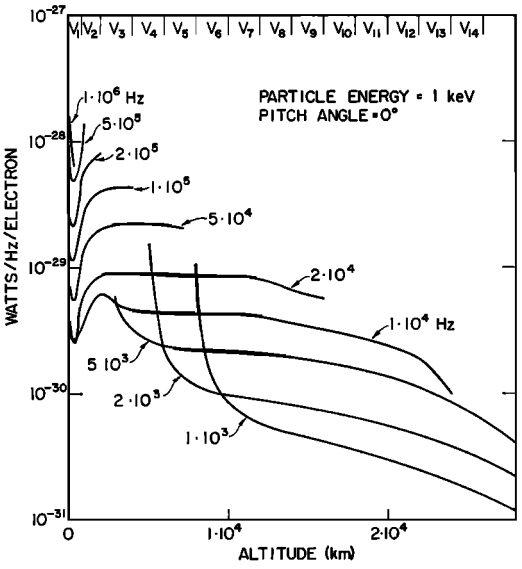

Fig. 10. The power generated at Cerenkov radiation by an electron with energy 1 kev and pitch angle 0° at frequencies between 1 kHz and 1 MHz as a function of altitude in the model region of generation.

At 1, 2, and 5 kHz, peaks are found at about 8000, 5000, and 3000 km, respectively. The peaks occur where the wave frequency is equal to the lower hybrid resonance f_{LHR}. In the case study shown in Figure 10, Cerenkov radiation is also generated at frequencies below f_{LHR}, but the power is several orders of magnitude below the power generated above f_{LHR}, and so it is not shown in the figure. As a function of particle energy only, the power is found to vary inversely proportionally with the square root of the particle energy in the energy range studied, that is for energies between 1 and 20 kev.

We will now attempt to calculate the total power produced by Cerenkov radiation in the model region of generation, that is, in a flux tube with the cold plasma properties and the energetic electron characteristics as discussed in section 3. The cross-sectional area of the tube at the bottom of the ionosphere is chosen to be 1 m², and we will calculate the total radiation produced below an altitude of 26,000 km. This last figure is rather arbitrary and mainly chosen because it is realized that the percentage deviation of the values of plasma and gyrofrequency in the model ionosphere (Figure 6) from the values in a real ionosphere probably is increasing with altitude, and that great errors thus may be made by including calculations at very high altitudes in the total power calculation. Also at about that altitude the cold plasma density is comparable to the energetic particle density, which means that the average temperature of the plasma is too high for the cold plasma theory to be valid.

For the purpose of the numerical integration of all the radiation produced, the flux tube is divided into 14 regions, the altitude boundaries of which are indicated in the top of Figure 10, and it is then assumed that the power produced in any of these regions by an electron with a certain energy and pitch angle is the same everywhere in the region, but usually different from one region to another. The total volume of the tube of lines of force is found to be 1.1×10^9 m³.

As mentioned above, the power generated is inversely proportional to the square root of the particle energy, with all other parameters being constant, but for ease of numerical power integration, we will take the power to be independent of energy within each of the 5 energy intervals shown in Figure 8. Finally, because the power generated has been found to be rather insensitive to pitch-angle variations except for large pitch angles, we will assume that the power is independent of pitch-angle variations.

With these assumptions the total power generated at a certain frequency now can be calculated by the following expression:

$$\begin{aligned}\sum \frac{dP}{df} = {} & V_1 \cdot \left[N(\Delta E_1) \cdot \frac{dP}{df} (\Delta E_1, V_1) \right. \\ & \left. + \cdots + N(\Delta E_5) \cdot \frac{dP}{df} (\Delta E_5, V_1) \right] \\ & + V_2 \cdot \left[N(\Delta E_1) \cdot \frac{dP}{df} (\Delta E_1, V_2) \right. \\ & \left. + \cdots + N(\Delta E_5) \cdot \frac{dP}{df} (\Delta E_5, V_2) \right] \\ & - - - - - - - - \\ & + V_{14} \cdot \left[N(\Delta E_1) \cdot \frac{dP}{df} (\Delta E_1, V_{14}) \right. \\ & \left. + \cdots + N(\Delta E_5) \cdot \frac{dP}{df} (\Delta E_5, V_{14}) \right]\end{aligned}$$

where V_n is the volume of the nth region of the flux tube (Figure 10), $N(\Delta E_n)$ is the density of energetic electrons in the nth energy interval (Figure 8), and dP/df $(\Delta E_n, V_m)$ is the power produced by an electron belonging to the energy interval ΔE_n in region V_m.

The total power generated in the model region we are considering has been calculated at a number of frequencies between 1 kHz and 1 MHz by the method described. The results obtained for the frequecy range between 1 and 100 kHz may be found from Figure 11 by multiplying the ordinate by 1 m², which represents the cross-sectional area of the base of the flux tube. The results of the calculations between 0.1 and 1 MHz are not shown in the figure, but if plotted they would appear as a continuation of the 'straight line' between 10 and 100 kHz.

To explain the noise spectral densities observed on the ground and from satellites (Figures 2 and 3), the total calculated energy, or at least a great part of it must propagate along the field lines and cross the 1-m² area bottom of the model region of noise generation. Whether this is likely to happen or not will be discussed as follows.

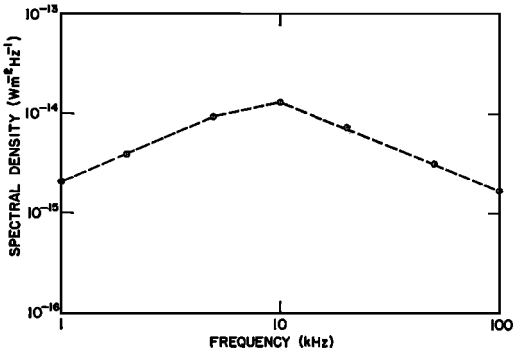

Fig. 11. Theoretical hiss spectrum in the lower ionosphere produced by Cerenkov radiation in the model region of generation.

There are two different mechanisms by which electromagnetic energy propagating in the whistler mode may be guided in the direction of the static magnetic field. One is called magnetoionic guiding. It is due to the anisotropy of a homogeneous plasma introduced by the presence of a static magnetic field. The other mechanism of guiding is called ducting, which can occur when field-aligned irregularities are present.

As the magnetoionic guiding is far too ineffective to explain the guiding needed in our case, and further because there is strong evidence that field-aligned irregularities exist in the auroral ionosphere, we will here only consider ducting as a possible mechanism for the guiding of the Cerenkov radiation-produced energy down to the bottom of the ionosphere.

Ducting of whistler-mode energy has been studied theoretically by several workers using different techniques. *Smith et al.* [1960] used ray theory, *Voge* [1962], *Booker* [1963], and *Walker* [1966] used mode theory, and *Adachi* [1965, 1966] applied a full wave theory to the problem. We will not discuss here the duct theories in any detail, but just note that the different workers in the field agree that a complete trapping of waves may take place depending on the type of irregularity. It is amazing that the enhancement or depression of the electron concentration needed for trapping to occur

is found to be only a few per cent or in some cases even less than 1%.

As mentioned in section 2, it has been observed by means of the Explorer 20 satellite [*Lund et al.*, 1967] that the auroral precipitation, which in this paper is considered as the source of high-latitude hiss, produces large electron concentration fluctuations within the latitudinal region containing the precipitation, and that the electron number density is increased at all altitudes between the F-layer maximum and the height of the satellite (about 1000 km). Very steep latitudinal electron concentration gradients are also found by *Calvert* [1966] to occur in the topside F layer at high latitudes. The gradients are often larger than 60% km^{-1} within the auroral zone.

It is not known if these irregularities extend along the field lines up to altitudes of several thousand km, but if they do, it seems very likely that wave guiding can take place.

If the field-aligned irregularities are produced at altitudes below 1000 km, the diffusion velocity v along the field lines can be estimated using the expression $\frac{1}{2}mv^2 = 3/2\ kT$, where m is the ion mass and T the ion temperature. Ion temperatures of about 6000°K have been measured by *Knudsen and Sharp* [1967] in the auroral zones, and using this figure and the mass of a proton a diffusion velocity of 10^4 m/sec is found. This means that the irregularities may diffuse up to an altitude of 10,000 km in about 15 minutes. Because the ion temperature probably is higher inside the region of auroral precipitation, where the electron concentration is high, it might be expected that the scale height would be larger here, and that the magnitude of the horizontal electron concentration gradient will increase with altitude.

Support of the hypothesis of ducting is provided by noise observations reported by *Heyborne* [1966]. By means of the OGO 2 satellite, noise at 17.8 kHz was regularly observed at auroral latitudes, and very often the noise amplitude changed by more than 40 db, while the satellite was moving only a few degrees in latitude. These observations indicate that the satellite moved in and out of the ducts in which the noise was trapped.

Thus there is strong evidence of ducting of whistler mode energy in the auroral ionosphere, and we will therefore assume that a large amount of the energy generated by the Cerenkov process is propagating in a flux tube down to the bottom of the ionosphere. Under the assumption of perfect guiding of the energy calculated above, the spectral density of the noise in the lower ionosphere would be as shown in Figure 11. It is rather similar to the noise spectra observed on the ground (Figure 2) and from a satellite (Figure 3), and it may be concluded that Cerenkov radiation from electrons with energies of a few kev seems to offer an explanation of the high-latitude noise phenomenon known as auroral hiss and polar LHR noise.

5. Summary

Observations of wideband high-latitude noise emissions in the VLF and LF ranges carried out from Byrd Station in the southern auroral zone and from the polar-orbiting satellite OGO 2 have been reported.

It is found that the typical noise spectra observed from the ground and in space exhibit similar characteristics with a peak spectral density near 10 kHz, and the spectral density falling off at both sides of the peak with about 20 db/decade. Maximum spectral densities observed on the ground and in space are about 10^{-14} and 10^{-13} w m^{-2} Hz^{-1}, respectively, but usually the peak spectral densities observed are one or two orders of magnitude lower. The lower spectral densities observed on the ground compared to those in space are probably due to absorption and/or internal reflection in the ionosphere.

Cerenkov radiation in the whistler mode from electrons with energies of a few kev in the high-latitude magnetosphere has been studied, and it is found that a calculated noise spectrum as produced by an incoherent Cerenkov process is comparable in magnitude and shape to observed noise spectrums.

The difference of about two orders of magnitude between the maximum observed spectral density (10^{-13}w m^{-2} Hz^{-1}) and the maximum calculated spectral density (10^{-14} w m^{-2} Hz^{-1}) is not considered serious for the following reasons: The calculated spectrum is produced by electrons with energies above 1 kev only, because the present knowledge of auroral electrons with energies below 1 kev is poor. Inclusion of electrons with energies below 1 kev in the calcula-

tion of the noise spectrum will increase the spectral density. Furthermore, the observed spectral densities probably are too high owing to the assumption in section 2 of longitudinal propagation. With wave normal angles other than zero, the refractive index will increase and the spectral density will therefore decrease.

It is concluded that the emissions known as auroral hiss and polar lower hybrid resonance noise may be generated by an incoherent Cerenkov process. This result is in contrast to earlier work by *Ellis* [1957], *Liemohn* [1965] and others, and is due to the improved model of generation used in this paper.

Acknowledgments. The author wishes to express his gratitude to all his co-workers at the Radioscience Laboratory, Stanford University, and in particular to Doctors R. A. Helliwell and T. F. Bell for helpful criticism.

The research reported in this paper was supported in part by the Office of Antarctic Programs of the National Science Foundation under grant GA-214 and in part by the National Aeronautics and Space Administration under contract NAS 5-3093.

References

Adachi, S., Study on the guiding mechanism of whistler radio waves, *Radio Sci., 69D,* 493, 1965.

Adachi, S., Theory of duct propagation of whistler radio waves, *Radio Sci., 1,* 671, 1966.

Allis, W. P., S. J. Buchsbaum, and A. Bers, *Waves in Anisotropic Plasmas,* The M.I.T. Press, Cambridge, Massachusetts, 1963.

Beghin, C., Ion-electron distribution in the upper ionosphere above the *F*2 peak at low and middle latitudes as deduced from whistler observations, in *Electron Density Profiles in the Ionosphere and Exosphere,* edited by J. Frihagen, p. 587, North-Holland Publishing Company, Amsterdam, 1966.

Booker, H. G., Guidance and beaming in the magnetosphere at hydromagnetic, audio, and radio frequencies, paper presented at General Assembly of URSI, Tokyo, Japan, 1963.

Calvert, W., Steep horizontal electron-density gradients in the topside *F* layer, *J. Geophys. Res., 71,* 3665, 1966.

Dowden, R. L., A theoretical model of electron density distribution along a geomagnetic line of force in the exosphere, *J. Atmospheric Terrest. Phys., 20,* 120, 1961.

Ellis, G. R., Low-frequency radio emission from aurorae, *J. Atmospheric Terrest. Phys., 10,* 303, 1957.

Evans, D. S., Rocket observations of low energy auroral electrons, *NASA Rept. X-611-66-376, NASA/GSFC,* Greenbelt, Maryland, 1966.

Frank, L. A., Initial observations of low-energy electrons in the earth's magnetosphere with OGO 3, *J. Geophys. Res., 72,* 185, 1967.

Gurnett, D. A., A satellite study of VLF hiss, *J. Geophys. Res., 71,* 5599, 1966.

Gurnett, D. A. and B. J. O'Brien, High-latitude geophysical studies with satellite Injun 3, 5, Very-low-frequency electromagnetic radiation, *J. Geophys. Res., 69,* 65, 1964.

Hagg, E. L., Electron densities of 8–100 electrons cm^{-3} deduced from Alouette II high-latitude ionograms, *Can. J. Phys., 45,* 27, 1967.

Helliwell, R. A., *Whistlers and Related Ionospheric Phenomena,* Stanford University Press, Stanford, California, 1965.

Helliwell, R. A., VLF noise of magnetospheric origin, paper presented URSI General Assembly, Munich, Germany, September 1966.

Heyborne, R. L., Observations of whistler-mode signals in the OGO satellites from VLF ground station transmitters, *Tech. Rept. 3415/3418-1,* Stanford Electronics Labs., Stanford University, Stanford, California, November 1966.

Hines, C. O., Heavy-ion effects in audio-frequency radio propagation, *J. Atmospheric Terrest. Phys., 11,* 36, 1957.

Jespersen, M., A. Haug, and B. Landmark, Electron density and collision frequency observations in the arctic *D* region, in *Electron Density Profiles in the Ionosphere and Exosphere,* edited by J. Frihagen, p. 27, North-Holland Publishing Company, Amsterdam, 1966.

Jørgensen, T. S., Morphology of VLF hiss zones and their correlation with particle precipitation events, *J. Geophys. Res., 71,* 1367, 1966.

Knudsen, W. C. and G. W. Sharp, Ion temperatures measured around a dawn-dusk-auroral-zone satellite orbit, *J. Geophys. Res., 72,* 1061, 1967.

Liemohn, H. B., Radiation from electrons in magnetoplasma, *Radio Sci., 69D,* 741, 1965.

Lund, D. S., R. D. Hunsucker, H. F. Bates, and W. B. Murcray, Electron number densities in auroral irregularities: Comparison of backscatter and satellite data, *J. Geophys. Res., 72,* 1053, 1967.

Mansfield, V. N., Cerenkov and cyclotron radiation as VLF emission sources, Radiophysics Lab., Thayer School of Engineering, Dartmouth College, Hanover, New Hampshire, 1964.

McEwen, D. J., and R. E. Barrington, Some characteristics of the lower hybrid resonance noise bands observed by the Alouette 1 satellite, *Can. J. Phys., 45,* 13, 1967.

McIlwain, C. E., Coordinates for mapping the distribution of magntically trapped particles, *J. Geophys. Res., 66,* 3681, 1961.

McKenzie, J. F., Cerenkov radiation in a magnetoionic medium (with application to the generation of low-frequency electromagnetic radiation in the exosphere by the passage of charged corpuscular streams), *Phil. Trans. Roy. Soc. London, A 255,* 585, 1963.

Smith, R. L., R. A. Helliwell, and I. W. Yabroff, A theory of trapping of whistlers in field-aligned columns of enhanced ionization, *J. Geophys. Res., 65,* 815, 1960.

Storey, L. R. O., A method to detect the presence of ionized hydrogen in the outer atmosphere, *Can. J. Phys., 34,* 1153, 1956.

Thomas, J. O., M. J. Rycroft, L Colin, and K. L. Chan, The topside ionosphere, 2, Experimental results from the Alouette 1 satellite, in *Electron Density Profiles in the Ionosphere and Exosphere,* edited by J. Frihagen, p. 322, North-Holland Publishing Company, Amsterdam, 1966.

Voge, J., Propagation guidée le long d'un feuillet atmosphérique ou (plus particulièrement) exosphérique, *Ann. Telecomm., 17,* 34, 1962.

Walker, A. D. M., The theory of guiding of radio waves in the exosphere, 1, Guiding of whistlers, *J. Atmospheric Terrest. Phys., 28,* 807, 1966.

(Received July 24, 1967.)